Twenty-Seventh Symposium (International) on Combustion/The Combustion Institute, 1998/pp. 2069–2076

PLANAR LASER-INDUCED FLUORESCENCE IMAGING OF CREVICE HYDROCARBON EMISSIONS IN A SPARK-IGNITED ENGINE

DAVID F. MARRAN,[1] MARSHALL B. LONG,[1] WILLIAM M. STUDZINSKI,[2] J. CHRISTIAN SWINDAL[2] AND WILLIAM P. ACKER[2]

[1]*Department of Mechanical Engineering and Center for Laser Diagnostics*
New Haven, CT 06520, USA
[2]*Texaco, Inc.*
Research and Development Department
Beacon, NY 12508, USA

In recent years, concerns over the impact of internal combustion engine hydrocarbon emissions on the environment have prompted tighter regulation on allowable emission levels. While much work has been done on reducing hydrocarbon emissions after they have entered the exhaust stream, less direct monitoring of the emission sources has been performed. An optically accessible four-stroke internal combustion engine was used to investigate how fuel composition and engine operating conditions affect hydrocarbon emissions. Various crevices, ranging in size from 1 to 2 mm, were simulated by drilling holes into a flat wall built into the head of the engine. Emissions from the residual fuel ejected by these crevices were directly monitored using planar laser-induced fluorescence (PLIF) from iso-octane/*n*-heptane fuel blends doped with 3-pentanone. The fluorescence was imaged at various times during the engine cycle and found to be extremely dependent on crevice size, engine load, and fuel reactivity. Under most normal load conditions, the largest crevice showed evidence of significant flame penetration, while flame penetration into the smaller crevices was found to vary with engine load. The results for the quench diameter were in good agreement with a simple crevice flame-quenching model. Fuels with lower octane ratings were shown to enhance flame penetration due to their increased reactivity.

Introduction

With the ever-increasing government-mandated restrictions on the emissions from internal combustion engines, it has become important to focus more attention on minimizing the sources of hydrocarbon emissions. Current technology relies on minimizing tailpipe hydrocarbon levels using catalytic conversion to complete the oxidation process begun in the engine. Although this approach has led to significant improvements in the steady-state tailpipe emission levels, future emissions standards will not be attainable using current technology postcombustion processing alone.

Much research has been done to locate the sources of hydrocarbon emissions within an engine, and agreement over the major sources has been reached [1–6]. Most unburned hydrocarbons are derived from fuel that is either packed into crevices, absorbed into oil layers, left unvaporized, leaked into the exhaust manifold, or left over from incomplete combustion. The dominant single source in a warmed-up engine is believed to be the crevices located within the cylinder, where almost 40% of the unburned hydrocarbons originate [2]. The top-land crevice is a major source of crevice emissions, and a number of studies have been undertaken in an attempt to minimize the emissions from this region [7–9]. During the engine cycle, the fuel-air charge is packed into these crevices as the pressure within the cylinder rises due to compression and the combustion process, and left largely unoxidized due to the quenching of the flame at the entrance of the crevice. As the pressure begins to drop within the cylinder, the unburned charge exits the crevice and enters the hot combustion products where a substantial fraction is oxidized.

To date, few studies have been undertaken to directly monitor crevice hydrocarbon emissions within operating engines [5,10–13]. Namazian and Heywood [5] have used spark Schlieren photography to image the flow out of crevices in an optically accessible square piston engine. This work indicated jet-like structures originating from the piston ring-gap region and spark plug threads. Medina et al. [11] used Raman scattering to monitor hydrocarbons exiting a simulated crevice built into an operating engine. More recently, planar laser-induced fluorescence (PLIF) imaging has been used to monitor crevice hydrocarbon emissions in both a direct-injection two-stroke engine [12] as well as a four-stroke engine [13]. Different studies have used fluorescence from the fuel itself [12,14,15] or fluorescence from various fluorescent tags added to the fuel in small concentrations [13,16–19]. Fluorescence from

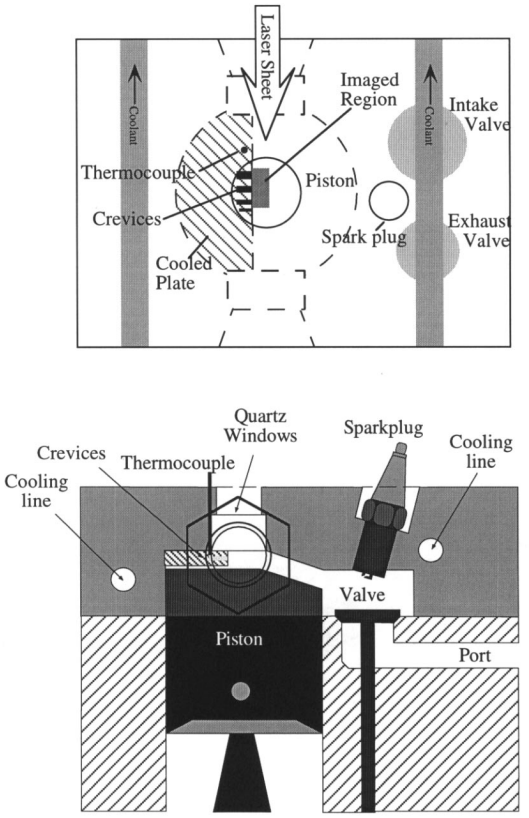

FIG. 1. Cross-sectional view of the modified Kohler "L-head" optically accessible engine. The top view of the engine head indicates the region imaged onto the CCD. The area monitored is 12.2 × 4.8 mm^2. Note the addition of several crevices within the window's field of view.

the fuel itself preserves the chemistry, but interpretation of the results may be biased by the unknown physical and optical properties of the fluorescing species in the fuel. Although fluorescent tags may alter the chemistry, knowledge of their thermophysical and fluorescence properties can provide useful insights into the phenomena being studied, such as the effect fuel volatility has on charge homogeneity [17] and crevice emission [19].

In the present work, emissions from several simulated crevices located within a four-stroke spark-ignited engine have been investigated using PLIF imaging from ketone-doped iso-octane/*n*-heptane fuel blends. The ketone used in this series of experiments was 3-pentanone, which has a vapor pressure almost identical to iso-octane and *n*-heptane [20]. In the first part of the study, outgasing from the different-sized crevices is characterized as a function of crank angle for a given engine load, wall temperature, and fuel composition. In the second part, the engine crank angle is fixed, and the effect of engine load on crevice emissions is characterized and compared to a simple crevice flame-quenching model. Finally, the impact of fuel reactivity on emissions is studied by changing the iso-octane/*n*-heptane ratio of the base fuel.

Optical Four-Stroke Engine

A schematic view of the engine used for this research is shown in Fig. 1. The design is based on a single-cylinder Kohler K-91 L-head that has been retrofitted with a specially designed aluminum head. This head has two 2.5-cm-diameter UV-grade quartz windows that permit the laser to pass through the engine, while a third 2.5-cm-quartz window located on top of the head allows imaging of the PLIF signal. In order to maintain the original compression in the cylinder (7.8:1), the piston has been extended with an aluminum cap. A brass plate containing a series of holes is used to simulate the crevices within an engine. This plate is bolted to the head such that the holes are within the field of view of the top window. Three crevices were investigated: 1.02-, 1.60-, and 2.06-mm-diameter holes, each 4.8-mm deep.

The original carburetor and ignition system have been replaced by computer-controlled fuel injection and ignition systems (Electromotive TEC-2). The computer maintains stoichiometric operation via closed loop control with a wide-band oxygen sensor located in the exhaust line. By operating the engine around stoichiometric, the buildup of soot deposits on the quartz windows is virtually eliminated, and the windows and crevices remain clean for an entire day of testing.

Engine speed is maintained at ~1120 rpm by driving the engine with an electric motor. The motor does an excellent job of maintaining engine rpm, resulting in <2% increase in rpm over an order of magnitude increase in throttle (3–31% of wide open throttle). The cylinder pressure is monitored using a piezoelectric pressure transducer (Kistler 6053B60), and the throttle is adjusted to stabilize the average engine pressure trace to match a reference condition recorded previously.

Laser-Induced Fluorescence Technique

The experimental configuration for the LIF study is shown in Fig. 2. The fourth harmonic of an Nd:YAG laser (266 nm, 3–120 mJ/pulse, 5 ns pulse width) is formed into a sheet that passes along the crevices within the engine. A thin sheet is formed using a single 30-cm quartz cylindrical lens. With this configuration, wall interferences are confined to the edge of the crevices, making it possible to obtain measurements extremely close to the crevice entrance.

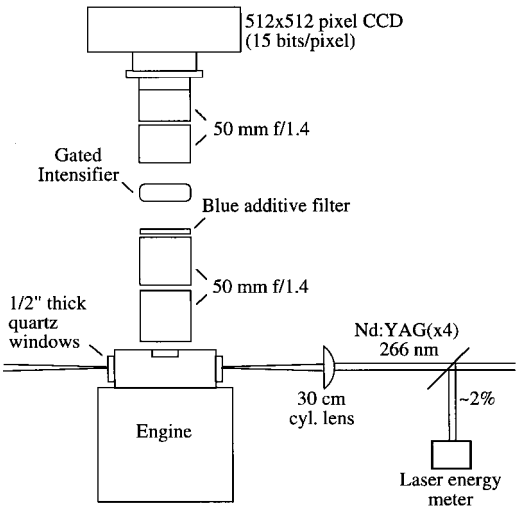

FIG. 2. Experimental setup for PLIF imaging of the ketone-doped fuels.

The fluorescence is imaged (1:1 magnification, $f/5.6$ optics) onto a gated microchannel plate image intensifier (DEP XX1450DH, 200-ns gate) using a pair of 50-mm camera lenses. A Rolyn blue additive filter (>70% transmission from 380 to 490 nm) minimizes interferences from wavelengths outside the ketone fluorescence range (300 to 550 nm, 420-nm peak). The image intensifier is optically coupled to a 512 × 512 pixel, 15-bit CCD camera (Princeton Instruments TE/CCD-512TKM). The images are binned 2 × 2 and cropped to 255 × 100 pixels. The area imaged within the engine covers 12.2 mm along the wall by 4.8 mm away from the wall (see Fig. 1). The pixel volume is 48 × 48 × ~200 μm^3 (estimated laser sheet thickness) for these data.

Synchronization of the laser and intensifier to the engine cycle is accomplished with a digital delay generator triggered by a shaft encoder coupled to the engine. The electronics can be configured for either single cycle or multicycle averaging on the CCD. When multicycle averages are taken, the measurement is repeated to ensure consistency in the data. The laser energy, cylinder pressure, and plate temperature are recorded along with the CCD images and stored by the computer for analysis.

In order to make the images quantitative, a background is subtracted to eliminate detector fixed-pattern noise, dark charge, and engine fluorescence interferences not related to the ketone fluorescence. This background is obtained by running the engine under identical load and crank-angle conditions as the data, but using propane as the fuel, which does not fluoresce. In order to account for the nonuniform detector response and laser sheet intensity profile, the data images are divided by a reference image obtained with a uniformly doped field of view. The reference image is taken under identical engine conditions as the data but during the compression stroke (70° BTDC, the point at which the cylinder pressure just begins to go above atmospheric prior to ignition, at 15° BTDC). Cycle-to-cycle charge inhomogeneity is accounted for by averaging 2640 engine cycles. A new reference image is obtained for every operating condition, which makes it possible to normalize for variations in charge density and doping level. Lastly, any change in laser energy from the reference images to the data images is taken into account.

In these data, the absolute ketone concentration in the reference image is not known, so the results are multiplied by an arbitrary scaling factor. Once corrected in this manner, a signal of 10,000 indicates the same fluorescence intensity as the reference image but not necessarily the same number density because the local conditions are not known for the data. However, because separate reference images are taken for every operating condition, the correction process makes it possible to compare different fuels or dopants in a quantitative manner.

Crevice Emissions during a Typical Engine Cycle

In an initial series of measurements, the crevice emissions were monitored as a function of crank angle. Single-shot fluorescence images show that the unburned fuel emitted by the crevices appears to do very little mixing with the hot cylinder gases. In work done by Namazian and Heywood [5], it was shown that the crevice gases were in thermal equilibrium with the crevice walls, so we expect the emissions near the wall to be substantially cooler than the cylinder gases and indicative of the crevice composition. The fuel used is based on a primary reference fuel (PRF) blended from 90% iso-octane/10% *n*-heptane (90 PRF) doped with 10% 3-pentanone by volume. The undoped fuel studied is rated as 90 octane.

Average pressure versus crank angle for the engine conditions investigated are shown in Fig. 3. Average outgassing from the different crevices was investigated as a function of crank angle by recording images every 10 crank-angle degrees from 30° to 270° ATDC (marked A and B in Fig. 3). Each image is an average of 2640 engine cycles, taken under "moderate" load (24% throttle, 12.75-barA peak pressure) with a 165°C wall temperature.

To best understand the image data, the average signal near the wall was measured in a region above each of the three crevices and plotted in Fig. 4 (the image from 190° ATDC is inset). Each measurement covers a 520 × 150 μm^2 region located 200 μm away from the wall and is centered along the crevice centerline (see Fig. 4 inset). This region was chosen to

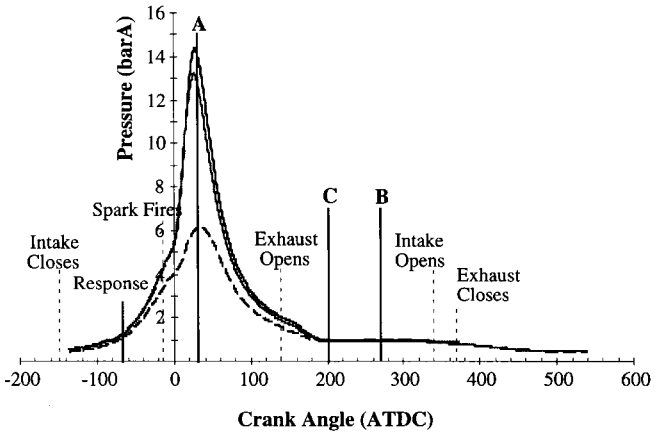

FIG. 3. Range of cylinder pressures studied. The three curves, from top to bottom, correspond to maximum load (31% throttle), moderate load (24% throttle), and minimum load (dashed, 3% throttle). Also indicated are the valve and spark timings, as well as the crank angles investigated.

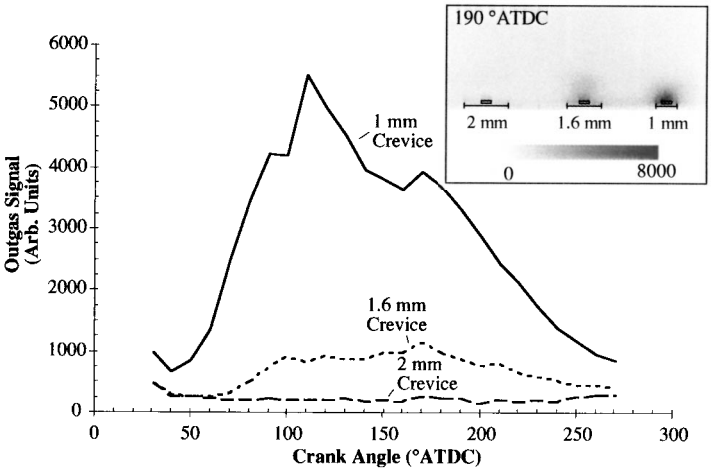

FIG. 4. Average emission levels measured 200 μm away from the wall, plotted as a function of crank angle. The inset shows the image used to calculate the emission at 190° ATDC. Also shown in the inset are the 520 $\times$ 150 μm^2 regions over which the emissions were averaged.

minimize the influence of the cylinder gases and wall interferences on the measurement region. It was found that choosing a smaller area did not alter the trends observed but did increase the scatter in the data.

As seen in Fig. 4, emission of unburned fuel begins just after the cylinder pressure peaks at 30° ATDC and continues throughout the exhaust stroke. The emission is largest for the 1-mm hole, indicating minimal flame penetration into that crevice. The fluorescence from this smallest hole peaks at two different crank angles, one before and one after the exhaust valve opens at 140° ATDC. The overall emission is driven by the difference in pressure between the crevice and the cylinder. It is believed that the small dip observed is caused by the sudden opening of the exhaust valve, which produces an initial burst of bulk fluid motion outside the crevice. This motion lowers the signal level by driving the crevice gases away from the front of the crevice but quickly returns as the motion within the cylinder moderates. The signal from the 1.6-mm hole has a lower overall signal level than the 1-mm crevice due to partial flame penetration and burnout of the fuel. Fluorescence from the 1.6-mm crevice begins slightly later in the cycle and does not show an initial peak. As will be shown, there is a significant amount of flame penetration into this crevice at this engine load, so the initial emissions will be dominated by combustion products rather than unburned fuel. In data where the engine load is reduced, two peaks appear for the 1.6-mm hole. On the other hand, the 2-mm hole shows very little emission, indicating almost complete penetration of the flame into the crevice.

In order to investigate the effects of engine load and fuel reactivity on the crevice outgassing, these data were taken at a single crank angle while other engine parameters were altered. Based on crank angle surveys obtained at several different loads and wall temperatures, all subsequent data were taken at 200° ATDC (marked C in Fig. 3). This angle gave strong fluorescence, low background interferences,

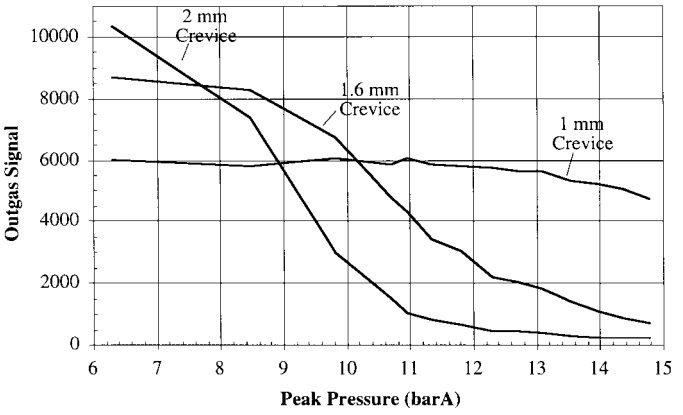

FIG. 5. Effect of peak cylinder pressure on crevice emission levels at 200° ATDC for 1130 rpm and 135°C wall temperature.

and avoided questions of the pressure dependence of the fluorescence signal, because the cylinder has returned to atmospheric pressure.

Effect of Engine Load on Crevice Emissions

An increase in engine load is expected to affect crevice hydrocarbon emissions in two ways: (1) increased cylinder gas temperatures and (2) increased cylinder pressure. The increase in cylinder gas temperatures will enhance the decomposition of hydrocarbons as they exit the crevices and will also raise the wall temperatures because of increased thermal loading. In our engine, the thermal loading effect was minimized by adjusting coolant flow rates to maintain a constant wall temperature (135°C) and coolant out temperature above the valves (70°C). Increased cylinder pressure alters crevice emissions by raising the number density of the fuel packed into crevices and by decreasing the flame quenching diameter (d_q = the smallest opening a flame can penetrate without extinction under a given set of conditions). The quench diameter is a strong function of the fuel, stoichiometry, crevice temperature, and cylinder pressure, but qualitative scaling laws permit reasonable modeling of the pressure effects [21].

Line plots corresponding to signal levels near the wall for a range of engine loads are shown in Fig. 5. Each data point is an average of over 7200 engine cycles and again covers 520 × 120 μm^2 centered 200 μm away from the crevice entrance. In the data, the abscissa is peak cylinder pressure, which is indicative of engine load (high engine load = high peak pressure). As mentioned earlier, each image acquired has been normalized by the signal at 70° BTDC, and backgrounds have been subtracted. The reference and data images are taken under the same load condition, so changes in charge density due to changes in load have been taken into account. The data show the expected trend with load: the flame can penetrate smaller crevices as the load increases. The flame enters the 2-mm crevice most easily, while the 1-mm crevice is left largely unpenetrated over a significant fraction of the load conditions monitored.

The classic model for flame penetration can be cast in the form of a scaling law based on the thermal diffusivity (α) and reaction rate of the fuel (RR) [21]:

$$d_q \propto \sqrt{\frac{\alpha}{RR}} \tag{1}$$

Because engine load is adjusted independently of wall temperature and engine rpm, we only need to characterize the effect of pressure (P) on the quench diameter. The thermal diffusivity scales as P^{-1}, and the reaction rate scales as P^{n-1}, where n corresponds to the order of the chemical reaction (~2 for hydrocarbons). As a result, we expect the quench diameter to scale roughly as P^{-1}, although this exponent is sometimes less than 1. Because of the coarseness of our measurements, the exponent will be assumed to be unity. For a given wall temperature, it should be possible to determine a calibration constant from the data that makes this scaling law quantitative:

$$d_q \approx \frac{C(T)}{P} \tag{2}$$

where P is the absolute pressure in the engine at the time the flame impinges on the crevice and $C(T)$ is constant for a given wall temperature. We expect $C(T)$ to decrease with increasing wall temperature because of reduced heat and radical loss to the walls. In the classic flame quench model, flame penetration is a step function—either the flame can penetrate the crevice or not. In the real case, when conditions are such that the quench diameter is close to a crevice diameter, the flame may be able to penetrate some distance before it is extinguished. In addition, instabilities in the engine operation will affect the quench diameter on a cycle-to-cycle basis. Because the data shown in Fig. 5 are an average over many engine cycles, a transition region occurs between the load at which the flame can just enter the

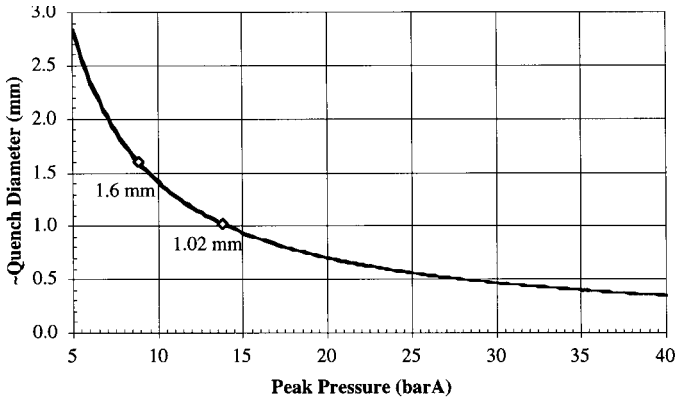

FIG. 6. Effect of peak pressure on quench diameter based on equation 2 with $C(T)$ estimated from the "90%" point of the data in Fig. 5. The diamonds correspond to the experimentally derived quench diameters of the 1.6- and 1.02-mm crevices.

crevice and the load where full penetration takes place. In Fig. 5, peak pressure was chosen along the abscissa because it is proportional to the change in load and is linearly proportional ($\pm 0.5\%$) to the cylinder pressure at which the flame first impinges on the crevice entrances.

$C(T)$ may be estimated for this wall temperature by defining successful flame penetration at some point in peak cylinder pressure versus emission curve for a given crevice size. For example, we chose to separate the "quenched and not quenched" regimes by finding the pressure at which the emission level has fallen to 90% of the maximum observed signal for a given crevice. With this in mind, the 90% point for the 1.6-mm crevice occurs at a peak pressure of 8.7 barA [$C(T) = 13.9$ barA mm], while the 1.02-mm crevice transition occurs at 13.4 barA [$C(T) = 13.7$ barA mm]. This scaling allows us to estimate the quench diameter for other load conditions, as depicted in Fig. 6. For example, the model predicts that any crevices smaller than ~0.4 mm will not permit significant flame penetration even under the highest loads (~35-barA peak pressure).

Flame penetration into the top-land crevice of an engine running under high-load conditions has been investigated indirectly by changing the diameter of the piston above the first ring and measuring the change in tailpipe hydrocarbon emissions [22]. Enlarging the top-land crevice clearance increased exhaust hydrocarbon emissions until a critical clearance was reached (~0.18 mm), at which time the flame was able to penetrate the crevice and reduce the emissions to the "zero" clearance level. Flame penetration into the top-land crevice can be considered equivalent to parallel plates, while the crevices used in our experiment are modeled using a circular duct. Flame quenching is controlled by heat and radical loss to the walls, while flame propagation occurs over a volume within the crevice. Neglecting end-wall effects, a circular duct of diameter d will have a surface area-to-volume ratio of $4/d$, while parallel plates with separation d will have a surface area-to-volume ratio of $2/d$. As a result, the quench diameter for a circular duct will be twice as large as the separation of parallel plates for identical conditions, that is, d_q (circular duct) $= 2d_q$ (parallel plates). With this scaling in mind, the 0.18-mm quench diameter measured by Haskell et al. [22] agrees well with the quench diameter estimated for our cylindrical crevice under the high-load limit (~0.4 mm). Our results are also in good agreement with the more recent work of Ishizawa [23].

Effect of Fuel Reactivity on Crevice Emissions

An important parameter expected to effect the hydrocarbon emissions is the reactivity of the fuel. This change in reactivity will affect the extent to which the flame enters a crevice because the quench diameter is related to the fuel reaction rate. In addition, an increase in reactivity should affect the post-flame oxidation process [24]. For the iso-octane/n-heptane fuel blends used in the present work, lowering the octane rating (i.e., increasing the concentration of n-heptane) increases the intermediate temperature reactivity of the fuel.

Four different octane fuels were made from blends of n-heptane and iso-octane (70%, 80%, 90%, and 100% by volume iso-octane) doped with 10% 3-pentanone. These fuels were studied under the same moderate engine load (24% throttle) used in the crank-angle survey. An average of 9900 engine cycles was taken for each condition, and the averaged region covers $520 \times 120\ \mu m^2$ centered 200 μm away from the crevice entrance. We know the 1.6-mm crevice is partially penetrated under this load condition, so the emission from it will be indicative of how fuel reactivity alters flame penetration. In fact, a strong trend is evident for this crevice: As octane rating is increased, the emission level increases. This is caused by a decrease in the reactivity that increases the quench diameter (from equation 1). This

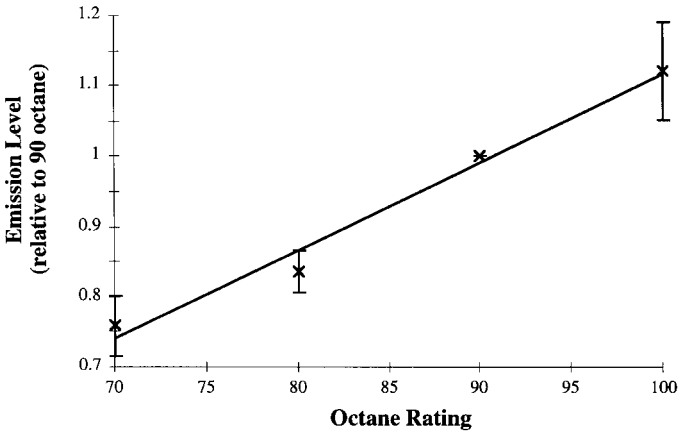

FIG. 7. Relative effect of octane rating on emissions from the 1.6-mm crevice, averaged over the entire wall-temperature range monitored (105–170°C). The data have been normalized using the 90% iso-octane case, and the error bars correspond to $\pm 1\ \sigma$ about the mean.

is clearly seen in Fig. 7, which plots the relative effect of octane rating on the emission level from the 1.6-mm hole, averaged over the entire wall-temperature range studied (105–170°C) and normalized using the 90% iso-octane case. The octane rating appears to have a linear effect on emissions over this range. The signal from the 1-mm hole shows the same general trend, but the different fuels are not as well separated. As mentioned previously, the flame is just barely able to penetrate the 1-mm crevice under these load conditions, so emissions from this crevice should be dominated by the postflame oxidation process. As a result, we can conclude that the fuel reactivity has only a modest effect on the postflame oxidation process. The trend observed is consistent with established flame quenching models; however, we are unaware of any other engine research that has investigated the correlation between fuel reactivity and crevice emissions.

Summary and Conclusions

The effects of various engine and fuel parameters on emissions from a series of circular crevices have been characterized in an optically accessible spark ignition engine using PLIF of various ketone-doped fuels. Hydrocarbon emissions from the crevices begin soon after the cylinder pressure peaks and persist throughout the entire expansion and exhaust strokes. The emission characteristics of different-size crevices depend on engine load, wall temperature, and fuel composition.

The effect of engine load on crevice emissions has been characterized for constant engine rpm and wall temperature. It was found that the penetration of the flame into the crevices was satisfactorily modeled using the approximate P^{-1} pressure dependence on quenching diameter. From these results, we determined that the flame is unable to penetrate the 1-mm crevice under the moderate load condition investigated in the later portions of the study. It was also found that the emission from this crevice is rapidly heated by the hot cylinder gases. These two results indicate that the emissions from this crevice provide insight into the cylinder-gas–crevice-emission interactions. The 1.6-mm crevice was significantly penetrated by the flame under the moderate load condition, and its signal can therefore be used to measure the degree of flame penetration as engine operating parameters are varied. Thus, the 1- and 1.6-mm crevices allow interpretation of the two different aspects of the crevice cycle: (1) flame penetration (1.6-mm crevice) and (2) postflame oxidation (1-mm crevice). The 2-mm crevice was almost completely penetrated by the flame under most of the load conditions studied, resulting in extremely small emission levels.

Fuel reactivity has been investigated by characterizing the effect of octane rating on the emission levels. A reduction in emission levels from the 1.6-mm crevice was observed as the octane rating was lowered from 100 to 70. Since the 1.6-mm crevice signal is largely dependent on the extent of flame penetration, the observed trend must be due to a decrease in the quench diameter, which is consistent with the expected reduction in quench diameter with increased fuel reactivity. The emissions from the 1-mm crevice for different octane ratings are not well separated. Since the signals from the 1-mm crevice are indicative of the crevice-emission–hot cylinder-gas interaction (and thus the postflame oxidation process), the results imply that fuel reactivity has a smaller effect on the postflame oxidation process.

Acknowledgment

The authors thank Dr. Michael Drake for helpful comments.

REFERENCES

1. Saika, T., Korematsu, K., and Kono, M., *Combust. Sci. Technol.* 108:279 (1995).

2. Cheng, W. K., Hamrin, D., Heywood, J. B., Hochgreb, S., Min, K., and Norris, M., SAE paper 93-2708.
3. Heywood, J. B., *Internal Combustion Engine Fundamentals,* McGraw-Hill, New York, 1988.
4. Adamczyk, A. A., Kaiser, E. W., and Lavoie, G. A., *Combust. Sci. Technol.* 33:261 (1983).
5. Namazian, M. and Heywood, J. B., SAE paper 82-0088.
6. Lorusso, J. A., Kaiser, E. W., and Lavoie, G. A., *Combust. Sci. Technol.* 25:121 (1981).
7. Freier, R. and Schelling, H., SAE paper 95-2309.
8. Alkidas, A. C., Drews, R. J., and Miller, W. F., SAE paper 95-2537.
9. Wentworth, J. T., *Combust. Sci. Technol.* 4:97 (1971).
10. Sterlepper, J. and Neuber, H.-J., SAE paper 94-1994.
11. Medina, S. C., Green, R. M., and Smith, J. R., SAE paper 84-0378.
12. Drake, M. C., Fansler, T. D., and French, D. T., SAE paper 95-2454.
13. Green, R. M. and Cloutman, L. D., SAE paper 97-0823.
14. Winklhofer, E., Philipp, H., Fraidl, G., and Fuchs, H., SAE paper 93-0871.
15. Andresen, P., Meijer, G., Schlüter, H., Voges, H., Koch, A., Hentshecl, W., Oppermann, W., and Rothe, E., *Appl. Opt.* 29:2392 (1990).
16. Johansson, B., Neij, H., Aldén, M., and Juhlin, G., SAE paper 95-0108.
17. Swindal, J. C., Dragonetti, D. P., Hahn, R. T., Furman, P. A., Studzinski, W. M., Paggi, R. E., Sung, R. L., and Acker, W. P., SAE paper 95-0106.
18. Arnold, A., Becker, H., Suntz, R., Monkhouse, P., Wolfrum, J., Maly, R., and Pfister, W., *Opt. Lett.* 15:831 (1990).
19. Swindal, J. C., Furman, P. A., Loiodice, M. E., Stevens, R. W., Liu, P. C., and Acker, W. P., SAE paper 97-0825.
20. Smith, B. D. and Srivastava, R., *Thermodynamic Data for Pure Compounds, Part A, Hydrocarbons and Ketones,* Elsevier, New York, 1986.
21. Glassman, I., *Combustion,* 3rd ed., Academic, Orlando, 1996.
22. Haskell, W. W. and Legate, C. E., SAE paper 72-0255.
23. Ishizawa, S., in *Twenty-Sixth Symposium (International) on Combustion,* The Combustion Institute, Pittsburgh, 1996, pp. 2605–2611.
24. Kaiser, E. W., Siegl, W. O., Henig, Y. I., Anderson, R. W., and Trinker, F. H., in *Symposium on Mechanisms and Chemistry of Pollutant Formation and Control from Internal Combustion Engines,* Washington, D.C., August 23–28, 1992, American Chemical Society.

COMMENTS

Charles Westbrook, Lawrence Livermore National Laboratory, USA. Your study uses octane number as a measure of fuel reactivity for fuel exiting the simulated crevice. Because octane number is defined only in terms of relative autoignition and knocking tendency, I am not sure it is an appropriate measure for reactivity in your circumstances. Can you comment?

Author's Reply. To characterize the effect of reactivity, fuel blends of 70–100% iso-octane in *n*-heptane were used (denoted 70 = AD 100 octane). The laminar flame speed of iso-octane is less than that of *n*-heptane, and the blending of the two will result in an effective flame speed that is somewhere between the pure compounds. Because the quench diameter is inversely proportional to the laminar flame speed (Ref. [21] in the paper), the quench diameter (and thus the emission levels) are expected to increase with the percentage of iso-octane.

•

John B. Heywood, MIT, USA. The exhaust blow-down process will be completed before 200° ATC, the point in the cycle where you have done much of your data analysis. The pressure to ratio, exhaust valve opening cylinder pressure to pressure at 200° ATC, will vary with engine load as well the fraction of the in-cylinder mass exhausted by 200° ATC. Thus, you will be looking at gas that went into the crevice at different times and penetrated the crevice to different depths, as load is varied. Did you consider this effect of load in your interpretation of your data?

Author's Reply. It would be interesting to measure crevice hydrocarbon emissions as a function of load for constant pressure ratio or constant fraction of in-cylinder mass exhausted, but that was not done in the present study. It is our feeling that the trends in the data would be largely the same, because measurements at 200° ATDC probe the material contained near the bottom of the crevice. Additionally, this crank angle has the advantage that the cylinder pressure is close to atmospheric. All gases in the measurement volume should have originated from the crevice and should be close to thermal equilibrium with the wall (Ref. [5] in the paper). Performing measurements at this crank angle also helps to eliminate density effects and changes in fluorescence yield caused by variations in the cylinder pressure with load.